



## Effect of BaTiO<sub>3</sub> nanoparticles contents on piezoelectric response of PVDF-BaTiO<sub>3</sub> nanocomposite

Vida Fathollahzadeh<sup>1</sup>, Mehdi Khodaei<sup>1,2,3\*</sup>

<sup>1</sup>Faculty of Materials Science and Engineering, K. N. Toosi University of Technology, Tehran, Iran;

<sup>2</sup>Materonics and Materionics Research Group, K. N. Toosi University of Technology, Tehran, Iran;

<sup>3</sup>Advanced Materials and Nanotechnology Research Lab, Faculty of Materials Science and Engineering, K. N. Toosi University of Technology, Tehran, Iran;

Received: 19 September 2023; Accepted: 17 December 2023

\*Corresponding author email: [khodaei@kntu.ac.ir](mailto:khodaei@kntu.ac.ir)

### ABSTRACT

The effect of content in the piezoelectric response of poly (vinylidene fluoride) (PVDF)/BaTiO<sub>3</sub> nanocomposites has been investigated in this work. The morphology of PVDF-BaTiO<sub>3</sub> composite films was characterized using scanning electron microscopy (SEM). Fourier transforms infrared (FTIR) spectroscopy and X-ray diffractometry (XRD) were used to investigate the phase analysis of samples. Voltage output increases significantly with increasing filler content. The electroactive  $\beta$ -phase of PVDF is nucleated by the presence of the ceramic filler, the effect being strongly dependent on filler content. The results revealed that incorporating the functionalized BaTiO<sub>3</sub> nanoparticles within the PVDF layer increases the piezoelectric response of pure PVDF compared to the sample with incorporated pure sample. Increasing concentration caused enhanced piezoelectric response.

**Keywords:** Barium titanate (BTO), Piezoelectric, nanoparticle, Polyvinylidene fluoride (PVDF).

### 1. Introduction

A lot of important ferroelectric materials are polar oxides, such as barium titanate (BaTiO<sub>3</sub>), lead zirconate titanate (Pb(Zr, Ti)O<sub>3</sub>), and SrBi<sub>2</sub>Ta<sub>2</sub>O<sub>9</sub> [1]. These materials possess spontaneous polarization and great interest due to their unique properties. For example, barium titanate (BaTiO<sub>3</sub>) is a well-studied ferroelectric material with applications in capacitors, actuators, and sensors [2]. The ceramic substance known as BaTiO<sub>3</sub> has both piezoelectric and ferroelectric characteristics, and

it undergoes crystallization in a perovskite structure [3]. The material can display several crystal structures, including crystalline, hexagonal, cubic, tetragonal, orthorhombic, monoclinic, and rhombohedral, which are contingent upon temperature variations [4].

It is worth noting that, besides oxide ceramics, certain polymers also possess this specific property. Polyvinylidene fluoride (PVDF) is classified as a semicrystalline polymer due to the presence of amorphous chains that are interspersed among the

lamellar crystalline structures of the polymer matrix [5]. Polyvinylidene fluoride (PVDF) exhibits four distinct crystalline phases, which are contingent upon the specific processing conditions but only one out of four phases possesses piezoelectric properties [6].

Nanocomposite materials have garnered significant attention due to their potential to investigate the influence of small-scale material structures within a specific matrix [7]. Large amounts of research are being done on piezoelectric composites because they have better dielectric and electroactive properties than polymer matrices [8]. The PVDF/BaTiO<sub>3</sub> film is a composite material that used in various applications, including in the field of piezoelectric materials. Research has been conducted on the preparation and properties of this composite film. For instance, studies have investigated the influence of polarization intensity on the piezoelectric properties of the composite film [9]. Additionally, research has focused on the optimization of PVDF/BaTiO<sub>3</sub> nanocomposite thin films to enhance their functional properties [10]. It has been seen that adding BaTiO<sub>3</sub> causes the dielectric constant to rise, and this rise is directly related to the amount of filler [11]. The relationship between the dielectric constant and the rising BaTiO<sub>3</sub> concentration adheres to the theoretical framework proposed by the Yamada model [12]. The dielectric characteristics of BaTiO<sub>3</sub>/PVDF composites are influenced by both filler concentration and particle size [13]. This is attributed to the presence of space charge effects at the interface between BaTiO<sub>3</sub> and PVDF, as well as the domain configurations (single or multi-domain) of the BaTiO<sub>3</sub> powders.

This research primarily investigates the fabrication of BaTiO<sub>3</sub> nanoparticles with wet ball-milled nanocomposites. Additionally, PVDF/BTO composites were created using different concentrations of BaTiO<sub>3</sub>, which were prepared by solution casting. Sample characterization was examined through the employment of scanning electron microscopy (SEM), Fourier-transform infrared spectroscopy (FTIR), and measuring output voltage with a piezoelectric test.

## 2. Experimental section

### 2.1. Materials and Samples Fabrication

PVDF powder (CH<sub>2</sub>=CF<sub>2</sub>, MW= 275,000 g/mol; Kaynar 761) and BaTiO<sub>3</sub> commercial powder (Submicron size; Sigma-Aldrich) were the main components. N-Dimethylformamide (C<sub>3</sub>H<sub>7</sub>NO, DMF,

Merk) and 1H,1H,2H,2H-Perfluorodecyltriethoxysilane (FAS) (C<sub>16</sub>H<sub>19</sub>F<sub>17</sub>O<sub>3</sub>Si, FAS-17, Sigma-Aldrich) were used as the solvent material to dissolve PVDF/BTO composite and surface functionalization.

Wet ball-milling is widely accepted as an economical, simple, and highly effective technique for fabricating nanostructured and amorphous materials [14]. The procedure was begun by mixing the 2 gr of submicron sized BTO (mBTO) powder with 2 ml of ethanol at room temperature for 4 hours. When the fabrication of nanoparticles is finished, nanoparticles are functionalized [15] with fluoroalkylsilane (FAS) [16]. This process was performed in a Planetary ball mill (Amin Asia Fanavar, Iran). The milling media consisted of 40 gr zirconia balls confined in a 100 mL zirconia vial, which is selected because of avoiding the impurity induced during milling. The ball-to-powder weight ratio was 10:1 in all milling runs, and the vial rotation speed was 400 rpm. Following ball milling, the resulting solution was frozen and dried in a freeze dryer for one day to obtain the dried nanoparticles.

For film casting, ceramic nanoparticles F<sub>n</sub>BTO with different concentration (0, 5,10, 15% wt) of functionalized BTO nanoparticles (F<sub>n</sub>BTO)) were dispersed in 10 cc DMF by an ultrasound bath for 60 minutes. Then, 2 gr of PVDF was added to the solution and stirred in a magnetic stirrer containing oil bath equipped proportional integral derivative (PID) controller at 60 °C until complete dissolution of the polymer for, 60 minutes with 3.5 speed. Films were prepared by spreading the suspension on a glass plate with 0.3 cm height and placing it in a vacuum oven for 720 minutes at 60 °C.

### 2.2. Characterization

Samples were analyzed by X-ray diffraction method to figure out the crystalline phases using a X-ray diffractometer (XRD; Rigaku; Ultima IV) with a Cu radiation source (wavelength of 1.54 Å, 40 kV and 40 mA). A step size of 0.02° speed was used to record the diffraction intensity in the diffraction range of 5-80. Crystallite size and mean lattice strain (estimated by the Williamson–Hall method [17]) were calculated from the XRD patterns.

Fourier Transform Infrared spectrometer (FTIR; Thermo; Nicolet 380) was utilized to analyze the samples. The FTIR spectra were acquired within the spectral range of 400-4000 cm<sup>-1</sup>, employing a resolution of 2 cm<sup>-1</sup> and conducting 20 scans.

The morphology of the particles was analyzed using scanning electron microscopy (SEM; ZEISS Technology, EVO MA15) to observe the microstructure and element distribution, which accelerated at a voltage of 0.5–30 kV.

The samples were wrapped in aluminum foil in  $2 \times 2 \text{ cm}^2$  sizes for the piezoelectric test. The output voltage of the samples was measured by applying a force of 2.6 N and a frequency of 5 Hz using a homemade piezo-tester, which the details are presented elsewhere [18].

### 3. Results and discussion

#### 3.1 Fabrication of BaTiO<sub>3</sub> nanoparticles

Agglomeration of nanoparticles has occurred due to the high surface energy of the nanoparticles. Therefore, it needs to be functionalized. The morphology of nano functionalized particles of BaTiO<sub>3</sub> was investigated by SEM, and images at different magnifications are shown in Fig. 1a. The shape of the particles can be seen in both spherical and angular forms. Functionalization plays a crucial role in achieving uniform dispersion of nanoparticles in

a liquid. That helps to prevent the agglomeration or aggregation of nanoparticles by reducing the inter-particle forces and stabilizing the dispersion. This is particularly important for maintaining the stability and functionality of nanoparticles in various applications [19, 20]. SEM results BTO nanoparticles was done successfully and approximately size of nanoparticles was 120 nm.

The diagram in Fig. 1b shows that the peak broadening occurred in the FnBTO sample at an angle of 31 degrees compared to the BTO sample. Also, X-ray peaks are broadened for three reasons: a) particle size less than 100 nm b) strain in the structure c) device errors.

Besides the peak broadening factors mentioned above, other factors can also affect the broadening of powder diffraction pattern peaks. In milling, plastic deformation of particles occurs in micrometer dimensions, so the internal energy, density of dislocations, and other defects increase. Moreover, there is a change in the lattice parameter and the distance between the atomic planes. Therefore, it is challenging to determine the exact amount of

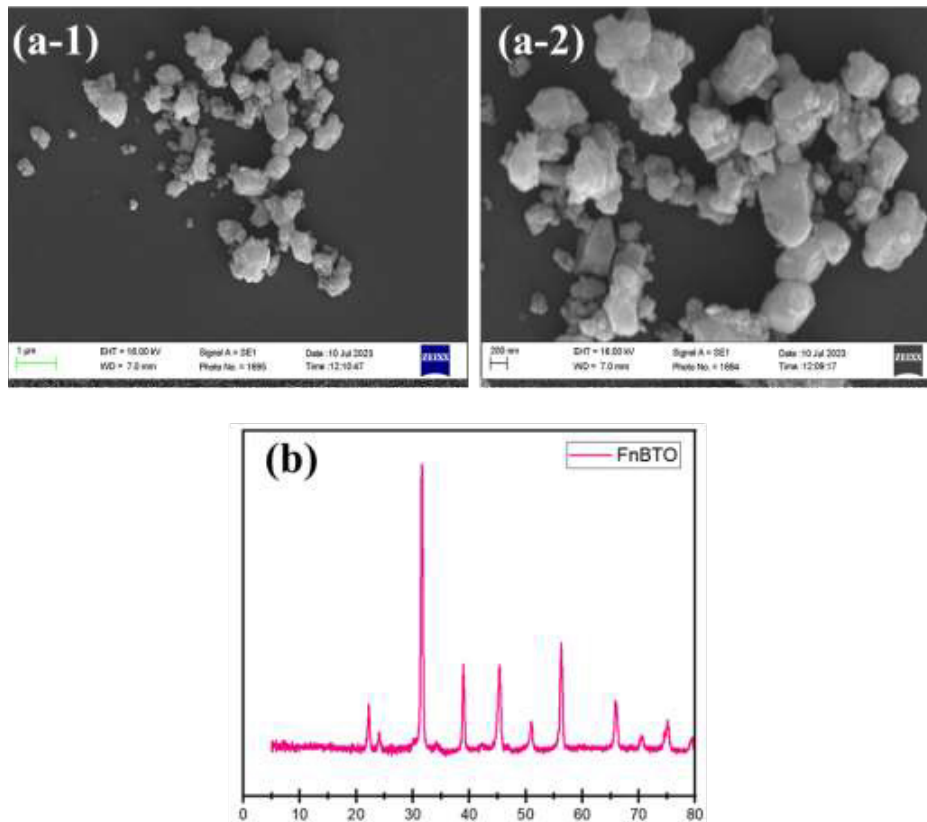


Fig. 1- SEM images of (a) FnBTO particles at several magnifications (b) X-ray diffraction (XRD) pattern analysis of FnBTO particles.

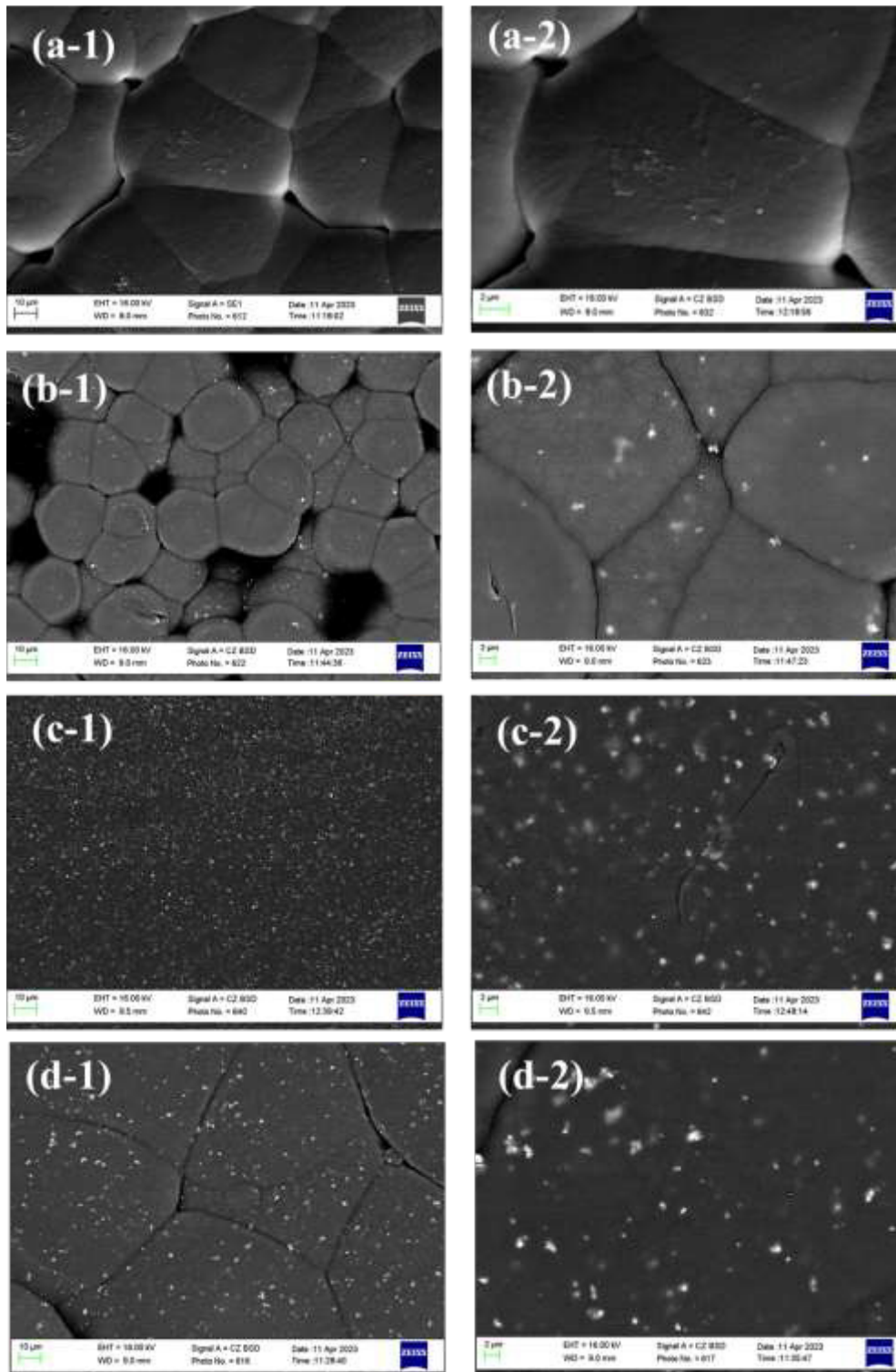


Fig. 2- SEM images of (a) PVDF film, (b) PVDF/ 5% wt F-nBTO composite film (c) PVDF/ 10% wt F-nBTO film (d) PVDF/ 15% wt F-nBTO film.

broadening in mechanical milling. The measured strain was equal to 0.57%, and the crystallite size was approximately measured by the Williamson-Hall method. The average size of the crystallites in F-nBTO was determined to be approximately 27 nm using the Williamson-Hal formula.

### 3.2. Fabrication of PVDF/ BaTiO<sub>3</sub> nanocomposite

Fig. 2c the PVDF matrix contains uniformly

distributed nanoparticles with no voids or cracks, while Fig. 2(a, b) shows PVDF film with many voids and aggregation particles. During the crystallization process, a spherical structure with small voids scattered between the spherical regions was formed, as shown in Fig. 2a-2 [21]. The spherulites grow and expand during crystallization by absorbing the liquid polymer phase that crystallizes in the inter-polymer area. At the final stage of the crystallization process, there is no liquid phase existing,

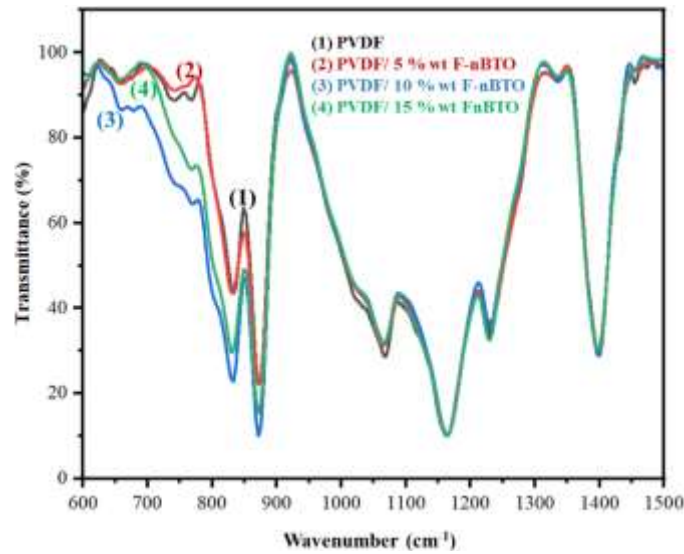


Fig. 3- FTIR-ATR spectra of F-nBTO/PVDF composite films.

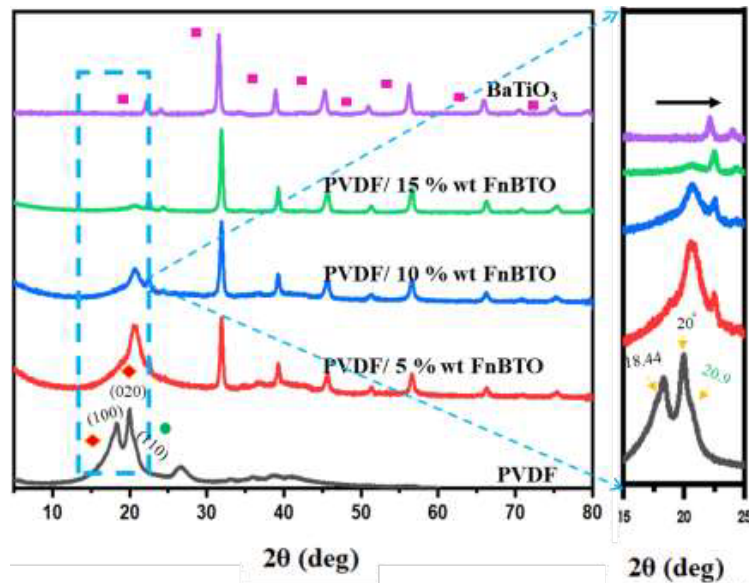


Fig. 4- X-ray diffraction pattern analysis of PVDF and PVDF/FnBTO nanocomposite films.

there are voids between the crystallized spherulites (Fig. 2a-1) [12]. The morphology of the PVDF film sample closely resembles that of  $\alpha$ -PVDF.  $\beta$ -PVDF samples have smaller spherulites and a porous structure compared to  $\alpha$  phase, resulting in weak mechanical properties [16]. The SEM images of the nanocomposite samples (Fig. 2c) reveal that the nanofillers (10% wt) are distributed effectively. SEM images shows that in 5% wt, it has voids like the pure sample, reduce the strength of the film. In the sample of 10 and 15% wt, no voids can be seen, but in the sample of 15%, the ceramic content is increased, and homogenous distribution does not take place.

The  $\beta$  phase was identified using infrared spectroscopy, primarily by observing the distinctive absorption band at 840 and 1279  $\text{cm}^{-1}$  wavenumbers. On the other hand, the  $\alpha$  phase can be identified by the presence of absorption bands at wavenumbers of 765, 795, 855, and 976  $\text{cm}^{-1}$  [22]. Fig. 3 dis-

plays the infrared spectrum of pristine  $\beta$ -PVDF for composites with different concentration of  $\text{BaTiO}_3$  particles. The presence of the  $\beta$  phase may be seen by the existence of the absorption band at 840  $\text{cm}^{-1}$  in all instances. Furthermore, the infrared spectra also exhibit an absorption band around 812  $\text{cm}^{-1}$ , which indicates the existence of minor quantities of  $\gamma$ -PVDF. Fig. 3, it is essential to acknowledge that the computation presented in this study does not consider the content of the  $\gamma$ -PVDF phase. The interaction between BTO particles and the PVDF matrix is also of significant importance in the crystallization process of PVDF, the ceramic filler plays the role of a nucleating agent for the  $\beta$  phase. As a result, the nucleation of BTO particles leads to the formation of more  $\beta$  phase, which can be seen in the 840  $\text{cm}^{-1}$  band in Fig.3. It has been shown that there is a positive correlation between the concentration of  $\text{BaTiO}_3$  particles and the rate of nucleation as shown in Fig. 3. increasing the concentra-

Table 1- Piezoelectric results of thin PVDF layer with different BTO concentrations

composites	Frequency (Hz)	Average sample output (mV)	applied force (N)	Sample sensitivity (mV/N)
PVDF	5	0.366	2.6	0.14
PVDF/ 5% F-nBTO	5	0.416	2.6	0.16
PVDF/10wt%F-nBTO	5	0.766	2.6	0.326
PVDF/15wt%F-nBTO	5	1.05	2.6	0.403

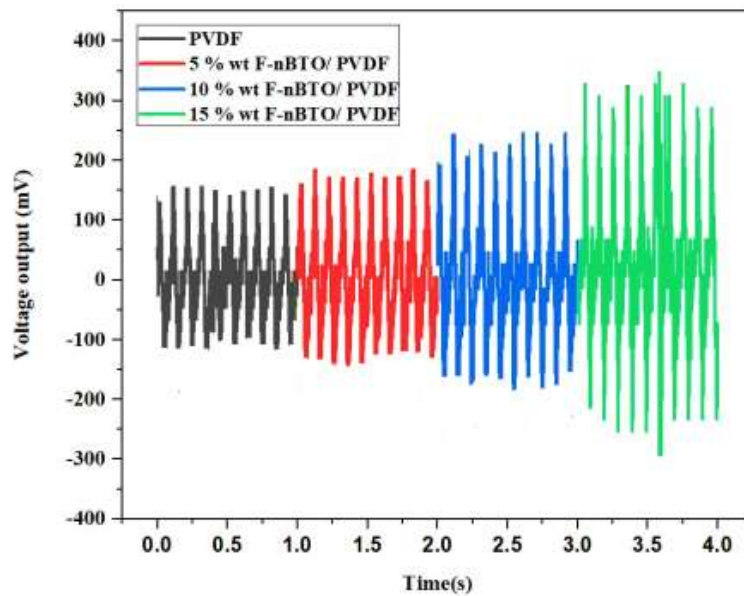


Fig. 5- plot of piezoelectric response of PVDF/BTO composite samples.

tion of BaTiO<sub>3</sub> caused the increase in the  $\beta$  phase.

Fig. 4 illustrates XRD patterns of PVDF and PVDF/FnBTO nanocomposite films. The peaks of FnBTO and PVDF in the composite films are separated, indicating that BTO is incorporated into the PVDF matrix without any other phase formation. Peaks in XRD for PVDF were found at 18.44 and 20 degrees, which correspond to the  $\alpha$  phase (Fig. 4). It shows the disappearance of this peak in nanocomposite films with the increase of BTO concentration, and the  $\alpha$  peaks have shifted to the right due to the strain caused by composites.

The output piezoelectric signals were carefully measured under stress conditions. The voltage responses of the film were plotted as a function of the force ranging from 2.6 N at a frequency of 5 Hz. The voltage output increases approximately by particle size decreases. Furthermore, the voltage sensitivity of film samples can be calculated for output voltage and force:  $S = V/F$ , where V and F are the corresponding variances in the output voltage signal and applied force. The measured values are given in the Table 1.

The addition of nBTO particles to the solution results in the formation of stronger O-H and F-C hydrogen bonds. This is likely due to the high polarity of hydroxyl groups. Ceramic nanoparticles serve as nucleating agents for PVDF crystals. At the

interfaces of PVDF/BTO particles, there are strong O-H and F-C hydrogen interactions and dipole interactions between PVDF and DMF solvents. These interactions tend to create CH<sub>2</sub>-CF<sub>2</sub> local dipoles packed in the TTT configuration characteristic of the  $\beta$  phase. So, adding BaTiO<sub>3</sub> as a filler in the PVDF matrix increases the output voltage (Table 2) [23]. In addition, increasing concentration of BTO nanoparticles caused increase piezoelectric response, as shown in Fig. 5.

#### 4. Conclusion

Composites PVDF containing BaTiO<sub>3</sub> particles nano-sized with concentrations (0, 5, 10, 15% wt) were prepared. The morphology investigation by SEM showed that the dispersion of 10 wt% nanoparticles within the PVDF matrix is better than of other concentrations. The results revealed that incorporating of the functionalized BaTiO<sub>3</sub> nanoparticles within the PVDF layer with vary concentration increase the piezoelectric in comparison to the sample with incorporated pure PVDF. On other hands, 15% wt of PVDF has maximum piezoelectric response.

#### Acknowledgments

The authors would like to thank Iran National Science Foundation (INSF) for financial supports to this work (INSF, Grant No. 4001120).

#### References

- Böttger U. Dielectric Properties of Polar Oxides. Polar Oxides: Wiley; 2004. p. 11-38.
- Martin LW, Rappe AM. Thin-film ferroelectric materials and their applications. *Nature Reviews Materials*. 2016;2(2).
- alasso FS, Kestigan M. Barium Titanate, BaTiO<sub>3</sub>. *Inorganic Syntheses*: Wiley; 1973. p. 142-3.
- Carter CB, Norton MG. *Ceramic Materials*. Springer New York; 2013.
- Nalwa HS. RECENT DEVELOPMENTS IN FERROELECTRIC POLYMERS. *Journal of Macromolecular Science, Part C: Polymer Reviews*. 1991;31(4):341-432.
- Gregorio JR, Cestari M. Effect of crystallization temperature on the crystalline phase content and morphology of poly(vinylidene fluoride). *Journal of Polymer Science Part B: Polymer Physics*. 1994;32(5):859-70.
- Sen M. *Nanocomposite Materials. Nanotechnology and the Environment*: IntechOpen; 2020.
- Safari A. Overcoming the limits of piezoelectric composites. *Natl Sci Rev*. 2023;10(9):nwad205-nwad.
- Li-zhu W, Chang-song Z, Chu W, Ru-peng W. The preparation of PVDF-BTO composite film and the influence of polarization intensity on the piezoelectric properties of composite film. *Journal of Physics: Conference Series*. 2021;1948(1):012191.
- Chauhan SS, Beigh NT, Mukherjee D, Mallick D. Development and Optimization of Highly Piezoelectric BTO/PVDF-TrFE Nanocomposite Film for Energy Harvesting Application. 2022 IEEE International Conference on Emerging Electronics (ICEE); 2022/12/11: IEEE; 2022.
- Muralidhar C, Pillai PKC. Effect on the melting point and heat of fusion of PVDF in barium titanate (BaTiO<sub>3</sub>)/Polyvinylidene fluoride (PVDF) composites. *Materials Research Bulletin*. 1988;23(3):323-6.
- Mendes SF, Costa CM, Caparros C, Sencadas V, Lanceros-Méndez S. Effect of filler size and concentration on the structure and properties of poly(vinylidene fluoride)/BaTiO<sub>3</sub> nanocomposites. *Journal of Materials Science*. 2011;47(3):1378-88.
- Fu J, Hou Y, Zheng M, Wei Q, Zhu M, Yan H. Improving Dielectric Properties of PVDF Composites by Employing Surface Modified Strong Polarized BaTiO<sub>3</sub> Particles Derived by Molten Salt Method. *ACS Applied Materials & Interfaces*. 2015;7(44):24480-91.
- Weissgaerber T, Kieback B. Dispersion Strengthened Materials Obtained by Mechanical Alloying - An Overview. *Materials Science Forum*. 2000;343-346:275-83.
- Huang, L., C. Lu, F. Wang, and X. Dong. Piezoelectric property of PVDF/graphene composite films using 1H, 1H, 2H, 2H-Perfluorooctyltriethoxysilane as a modifying agent. *Journal of Alloys and Compounds*, 2016. 688: p. 885-892.
- Khodaei M, Shadmani S. Superhydrophobicity on aluminum through reactive-etching and TEOS/GPTMS/nano-Al<sub>2</sub>O<sub>3</sub> silane-based nanocomposite coating. *Surface and Coatings*

Technology. 2019;374:1078-90.

17. Williamson GK, Hall WH. X-ray line broadening from filed aluminium and wolfram. *Acta Metallurgica*. 1953;1(1):22-31.

18. Sorayani Bafqi MS, Sadeghi A-H, Latifi M, Bagherzadeh R. Design and fabrication of a piezoelectric out-put evaluation system for sensitivity measurements of fibrous sensors and actuators. *Journal of Industrial Textiles*. 2019;50(10):1643-59.

19. Miyazawa T, Itaya M, Burdeos GC, Nakagawa K, Miyazawa T. A Critical Review of the Use of Surfactant-Coated Nanoparticles in Nanomedicine and Food Nanotechnology. *Int J Nanomedicine*. 2021;16:3937-99.

20. Morsy SM. Role of surfactants in nanotechnology and their applications. *Int. J. Curr. Microbiol. App. Sci*. 2014;3(5):237-60.

21. Sencadas V, Gregorio R, Lanceros-Méndez S.  $\alpha$  to  $\beta$  Phase Transformation and Microstructural Changes of PVDF Films Induced by Uniaxial Stretch. *Journal of Macromolecular Science, Part B*. 2009;48(3):514-25.

22. Nishiyama T, Sumihara T, Sasaki Y, Sato E, Yamato M, Horibe H. Crystalline structure control of poly(vinylidene fluoride) films with the antisolvent addition method. *Polymer Journal*. 2016;48(10):1035-8.

23. Walrafen GE. *Water: a comprehensive treatise*. by F. Franks, Plenum Press, New York. 1972;1:151.